Journal of Alloys and Compounds 488 (2009) 65–71

Contents lists available at ScienceDirect

Journal of Alloys and Compounds

journal homepage: www.elsevier.com/locate/jallcom

Quantification of the free volume in $Zr_{45.0}Cu_{39.3}Al_{7.0}Ag_{8.7}$ bulk metallic glasses subjected to plastic deformation by calorimetric and dilatometric measurements

Yue Zhang[a,b,*], Horst Hahn[a,b]

[a] Institute of Nanotechnology, Forschungszentrum Karlsruhe, PO Box 3640, D-76021 Karlsruhe, Germany
[b] Joint Research Laboratory Nanomaterials, Technische Universität Darmstadt, Petersenstr. 23, D-64287, Darmstadt, Germany

ARTICLE INFO

Article history:
Received 4 August 2009
Received in revised form 17 August 2009
Accepted 19 August 2009
Available online 27 August 2009

Keywords:
Free volume
Metallic glasses
Differential scanning calorimetry
Dilatometry
Zr–Cu–Al–Ag

ABSTRACT

$Zr_{45.0}Cu_{39.3}Al_{7.0}Ag_{8.7}$ bulk metallic glasses (BMGs) were prepared using suction casting technique. Plastic deformations were carried out by cold rolling and high-pressure torsion (HPT). The absolute contents of free volume in the as-cast, preheated and deformed samples were determined by differential scanning calorimetry (DSC) and dilatometry using the free volume model (FVM). The parameters required in the FVM are experimentally determined to be $b = 0.107$, $\beta = 642.1$ kJ/mol, $D^* = 10.3$ and $T_0 = 496.9$ K, respectively. The equilibrium free volume determined by these parameters is in good agreement with that calculated from previous enthalpy relaxation experiments, showing the reliability of the values of the parameters. It is found that the content of free volume in the as-cast sample is 0.533% with respect to the atomic volume of the BMG. The free volume in the HPT deformed sample is determined to be 0.672%, which is the largest among all the samples. The excess free volume introduced by cold rolling is found to increase with the deformation strain and show weak strain rate dependent behavior. Finally, attempts are made to simulate the experimental DSC curve using a bimolecular kinetics in the flow defect model. However, the result shows that the kinetics of free volume may be more complicated than as described as a bimolecular process.

1. Introduction

The research of free volume in metallic glasses (MGs) has drawn considerable attentions since the free volume model (FVM) was developed by Turnbull and Cohen [1–3]. The success of FVM in explaining many properties of MGs such as the viscosity [4], diffusivity [5], specific heat capacity [6] and plasticity [7] made this model widely acceptable. Recent results of molecular dynamic simulations have shown that the free volume is closely related to the structure of MGs [8–10]. Therefore, the quantification of free volume plays an important role on understanding the relationship between the structures and properties of MGs. There have been many approaches to quantify free volume in MGs experimentally using X-ray diffraction (XRD) [11], density measurements [12–14], positron annihilation spectroscopy (PAS) [15–17] or calorimetric measurements [6,18,19]. However, most of the studies were focused on the change in free volume during structural relaxation or crystallization, quantification of the absolute content of free volume in MGs remains still challenging.

Recently, a new family of Zr-based bulk metallic glasses (BMGs) in the Zr–Cu–Al–Ag system with excellent glass forming ability has been reported [20–23], which has promising applications in biomedical aspects due to Ni-free. Especially, $Zr_{45.0}Cu_{39.3}Al_{7.0}Ag_{8.7}$ was shown to have large plasticity among all the reported compositions. Therefore, quantifying the content of free volume and studying the evolution of free volume with temperature upon thermal treatments are of significant benefit to achieve a better understanding of this BMG from the aspects of both structure and properties.

In the present study, the absolute contents of free volume in the as-cast, preheated and plastically deformed $Zr_{45.0}Cu_{39.3}Al_{7.0}Ag_{8.7}$ BMG samples are quantified using calorimetric and dilatometric measurements within the framework of the FVM. The parameters in the FVM are determined experimentally by heating rate dependent glass transition, thermal expansion and specific heat capacity measurements, respectively. The evolution of the content of free volume with temperature in differential scanning calorimetry (DSC) scans is present.

2. Theoretical background

2.1. The evolution of free volume with temperature

It has been shown that the evolution of free volume with temperature during preparation and subsequent heating in a DSC scan

* Corresponding author at: Institute of Nanotechnology, Forschungszentrum Karlsruhe, PO Box 3640, D-76021 Karlsruhe, Germany.
E-mail address: yue.zhang@int.fzk.de (Y. Zhang).

0925-8388/$ – see front matter © 2009 Elsevier B.V. All rights reserved.
doi:10.1016/j.jallcom.2009.08.091

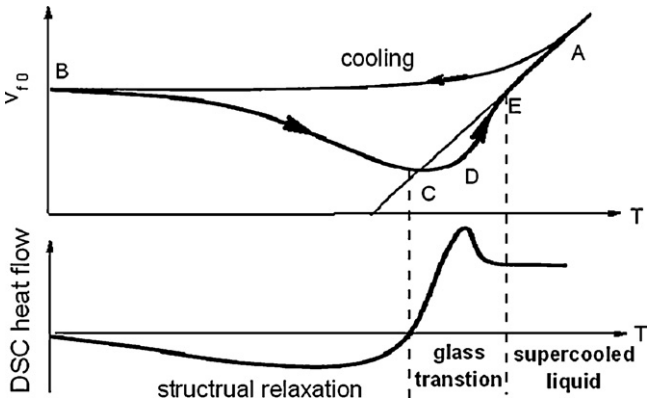

Fig. 1. A schematic drawing of the evolution of free volume with temperature.

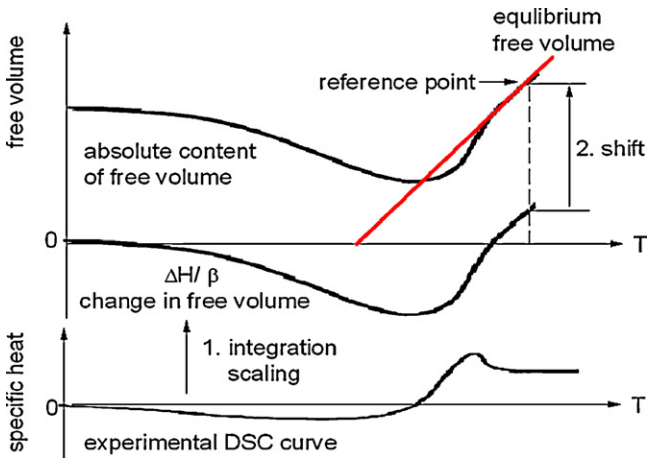

Fig. 2. A schematic drawing of the method used to calculate the absolute content of free volume. (1) An experimental DSC curve is firstly integrated and scaled to get the change in free volume; (2) the integrated curve is then shifted with reference of the equilibrium value of free volume in the supercooled liquid temperature range to get the absolute content of free volume.

can be described as follows (see Fig. 1) [6]: (1) the content of free volume in the supercooled liquid deviates from the corresponding equilibrium value (denoted by line AC) at the point A upon cooling, so a certain amount of excess free volume v_{f0} is trapped in the glass after preparation (curve AB); (2) upon heating the as-cast sample in DSC, the content of free volume decreases along curve BC and reaches an equilibrium value at temperature C; (3) from the point C on, the content of free volume increases along the curve CDE. However, it is smaller than the equilibrium value at the corresponding temperatures within the range of CE because of the sluggish mobility of atoms; (4) at the point E, the content of free volume reaches the equilibrium value again and then increases along line EA as long as the crystallization does not intervene.

2.2. The method of quantification of free volume

The quantification of free volume in the present study can be described by the following two steps:

(1) The experimental DSC curve is integrated to obtain the change in the enthalpy of the sample. By scaling the integrated curve with a coefficient β, the change in the content of free volume can be derived. This step is based on a simple assumption that the change in the enthalpy of the sample is proportional to the change in the content of free volume:

$$\Delta H = \beta \cdot \Delta v_f \tag{1}$$

where β is a coefficient with a dimension of energy, ΔH and Δv_f are the changes in the enthalpy and the change in free volume during the calorimetric measurements, respectively. Eq. (1) has been demonstrated via experiment by Slipenyuk and Eckert [24] in a $Zr_{55}Cu_{30}Al_{10}Ni_5$ BMG.

(2) The equilibrium values of free volume in the supercooled liquid range are employed as references to shift the scaled curve obtained in step (1), so that the absolute content of free volume can be determined (Fig. 2).

2.3. The determination of the parameters

Two quantities have to be known in order to calculate the absolute content of free volume, i.e. (1) the coefficient β in Eq. (1) to convert the change in the enthalpy into the change in the free volume and (2) the equilibrium value of free volume of the supercooled liquid to shift the curve of the change in free volume.

It has been shown that the equilibrium free volume can be formulated as [25]:

$$\frac{v_{feq}}{v_m} = \frac{b(T - T_0)}{(D^* T_0)} \tag{2}$$

where v_m is the atomic volume of the glass, b is a coefficient usually of the order of 0.1, T_0 is the Vogel–Fulcher–Tammann (VFT) temperature and D^* is the fragility parameter that depicts the deviation of the system from the Arrhenius relationship ($D^* \to \infty$). D^* and T_0 are usually determined by the viscosity measurements [26]. However, Busch et al. [27] suggested that the viscosity relaxation of the supercooled liquid and the heating rate dependent glass transition occur on same time scales. In the present study, D^* and T_0 are determined by the following relation:

$$\Phi = A \exp\left[-\frac{D^* T_0}{(T_g(\Phi) - T_0)}\right] \tag{3}$$

where Φ is heating rate used in the DSC scan, $T_g(\Phi)$ is the corresponding glass transition temperature at Φ, A is a fitting constant.

The difference between the thermal expansion coefficients of the supercooled liquid and the glass near the glass transition can be attributed to the production of equilibrium free volume in the glass transition range [6,25], which can be formulated as

$$3(\alpha_{sl} - \alpha_g) = \frac{d(v_{feq}/v_m)}{dT} = \frac{b}{(D^* T_0)} \tag{4}$$

where α_{sl} and α_g are the linear thermal expansion coefficients of the supercooled liquid and the glass, respectively. The value of b can be determined by substituting the values of D^* and T_0 into Eq. (4). Analogically, the difference between the specific heat capacities between the supercooled liquid and the glass near glass transition can be formulated as [6]:

$$C_{p,sl} - C_{p,g} = \frac{dH}{dT} = \left[\frac{d(v_{feq}/v_m)}{dT}\right] = \frac{\beta b}{(D^* T_0)} \tag{5}$$

where $C_{p,sl}$ and $C_{p,g}$ are the specific heat capacities of the supercooled liquid and the glass, respectively. The value of β can be obtained by substituting the values of b, D^* and T_0 into Eq. (5).

3. Experimental

$Zr_{45.0}Cu_{39.3}Al_{7.0}Ag_{8.7}$ master alloys were prepared by arc melting of the component elements with purities ranging from 99.9% to 99.999%. The master alloys were remelted five times under high purity argon (99.9999%) in order to achieve chemical homogeneity. Two kinds of BMG rods were prepared by suction the melt into water-cooled copper moulds, one is 4 mm in diameter (30 mm in length) and the other is 8 mm in diameter (10 mm in length). The surfaces of the rods were carefully polished after preparation. The compositions of the samples were checked by energy-dispersive X-ray spectroscopy (EDX, INCA) and only 0.3 at% deviation from the nominal composition was found.

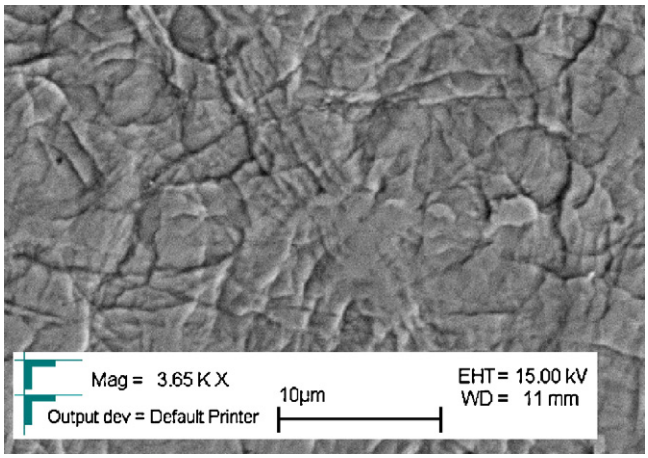

Fig. 3. The surface morphology of the $Zr_{45.0}Cu_{39.3}Al_{7.0}Ag_{8.7}$ sample deformed by cold rolling with $\varepsilon = 0.31$ at a strain rate of 4.6×10^{-3} s^{-1} examined by SEM, the shear bands can be clearly observed.

Disk shaped samples with a thickness of 0.86–0.9 mm were cut from the as-cast 4 mm diameter rod for cold rolling. The cold rolling was carried out using a conventional two roller mill (Bühler & Co) at ambient temperature. Repetitive rolling was performed without any metal sheets covered on both surfaces of the samples at different roller speeds of 1, 2 and 5 m/min, respectively. The corresponding strain rates were estimated to be 2.3×10^{-3}, 4.6×10^{-3} and 1.2×10^{-2} s^{-1}, respectively. High pressure torsion (HPT) deformation was performed on a self-built apparatus, where 0.4–0.5 mm thick disks cut from the as-cast 8 mm diameter rods were compressed between two pieces of rotating anvils at a pressure of approx 5 GPa, the total torsion angle (180°) was accomplished in two steps (90° × 2). The degree of deformation is characterized by the normal strain ε formulated as

$$\varepsilon = \frac{t_0 - t}{t_0} \quad (6)$$

where t_0 and t are the thicknesses of the sample before and after deformation, respectively. The glassy nature of the as-cast and deformed samples was verified by X-ray diffraction (XRD, Mo K_α radiation, Panalytical X'pert) and transmission electron microscopy (TEM, Tecnai F20, 300 kV). Scanning electron microscopy (Leo1525 FEG SEM, 15 kV) was used to examine the surfaces of the deformed samples.

Calorimetric measurements were performed using a DSC (Perkin-Elmer, Pyris 1) under a constant flow of high purity argon (99.9999%). The heating rate dependent glass transition measurements were carried out using disks cut from the 4 mm diameter as-cast with masses of approx 40 mg. A preheating treatment of all the samples used in this measurement was performed, i.e. the samples were firstly heated to 723 K at 0.33 K/s and were cooled to room temperature at 1 K/s after holding at 723 K for 60 s. All the samples can be thought to have the same content of free volume after the preheating treatment. The specific heat capacities of the as-cast, pre-heated and crystallized samples were determined by the ratio method described in Refs. [23,28] at 0.033 K/s using a sapphire standard as reference.

The linear thermal expansion coefficients of the as-cast, preheated and crystallized samples were measured by a dilatometer (Netzsch DIL402) from 328 to 700 K at a heating rate of 0.033 K/s under high purity helium (99.9999%). 4 mm diameter as-cast BMG rods with lengths of approx. 20 mm were used. The instrument was calibrated with a quartz standard at the same heating rate before the measurement was conducted. The preheating treatment was carried out using an infrared annealing furnace (Strohlein instruments, IR05, temperature accuracy ±5 K) under high purity argon with the same procedure used in the calorimetric measurements. Fully crystallized sample was obtained by isothermal annealing of an as-cast rod at 873 K for 3600 s. Surfaces of the samples were carefully polished after each heat treatment to remove any possible oxidation.

4. Results and discussion

Fig. 3 shows a representative surface morphology of the $Zr_{45.0}Cu_{39.3}Al_{7.0}Ag_{8.7}$ sample deformed by cold rolling with $\varepsilon = 0.31$ at a strain rate of 4.6×10^{-3} s^{-1} examined by SEM. The shear bands with an irregular pattern can be clearly observed, indicating the inhomogeneous deformation of the sample.

In Fig. 4 the glass transitions temperatures T_g of the pre-heated samples measured at various heating rates are present. In this study, T_g is taken to be the intersection of the two tangents, which is in coincidence with Ref. [27]. The thermal parameters including T_g, the crystallization temperature T_x and the crystallization enthalpy ΔH_x measured at these heating rates are listed in Table 1. It can be clearly seen that T_g shifts to higher temperatures as the heating rate increases. The fitting of T_g as a function of heating rate using Eq. (3) yields $A = 6.8 \times 10^9$, $D^* = 10.3$ and $T_0 = 496.9$ K (see Fig. 5). In addition, the heating rate dependent glass transitions in $Zr_{46.0}Cu_{39.3}Al_{7.0}Ag_{7.7}$ and $Zr_{60.6}Cu_{17.6}Ni_{10.0}Al_{9.8}Fe_{2.0}$ BMGs were also measured in order to evaluate the values of A, D^* and T_0 of $Zr_{45.0}Cu_{39.3}Al_{7.0}Ag_{8.7}$ BMG. The results of fitting are listed in Table 2 together with some literature values. It can be seen that all the values of D^* and T_0 obtained in the Zr-based BMGs in the

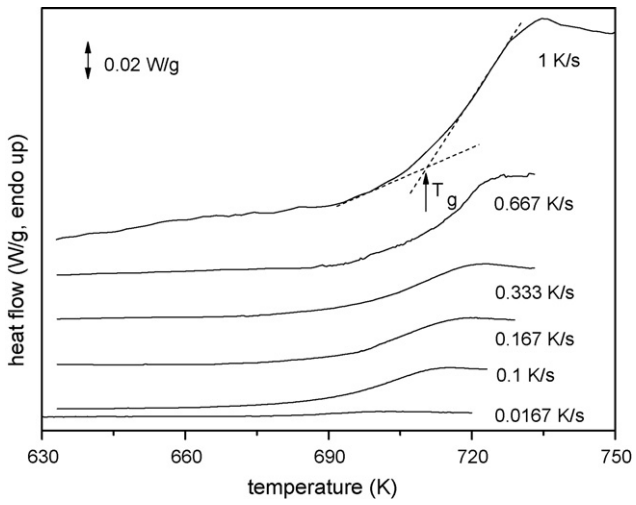

Fig. 4. The heating rate dependent glass transition of the preheated $Zr_{45.0}Cu_{39.3}Al_{7.0}Ag_{8.7}$ samples measured at various heating rates. The glass transition temperature is defined to be the intersection of the two tangents.

Table 1
The thermal parameters of the preheated $Zr_{45.0}Cu_{39.3}Al_{7.0}Ag_{8.7}$ samples measured at various heating rates.

Heating rate (K/s)	T_g (K)	T_x (K)	ΔH_x (kJ/mol)
0.0167	674.1	727.5	3.58
0.1	689.3	742.3	3.59
0.167	693.9	746.9	3.58
0.333	700.5	753.4	3.60
0.667	707.3	760.8	3.59
1	711.5	765.0	3.60
1.333	714.5	768.1	3.59

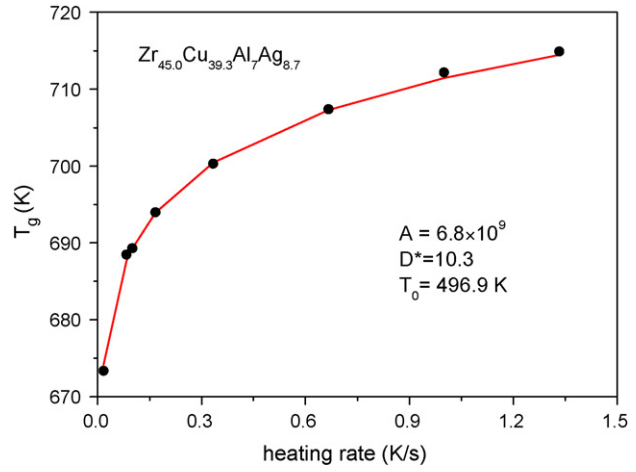

Fig. 5. The fitting of the glass transition temperatures as a function of the heating rates using Eq. (3).

Table 2
The values of A, D^* and T_0 obtained by fitting of the glass transition temperatures as a function of the heating rates using Eq. (3) together with some literature values.

BMGs	A	D^*	T_0 (K)	Ref.
$Zr_{45.0}Cu_{39.3}Al_{7.0}Ag_{8.7}$	6.8×10^9	10.3	496.9	This work
$Zr_{46.0}Cu_{39.3}Al_{7.0}Ag_{7.7}$	7.2×10^9	12.5	479.4	This work
$Zr_{46.0}Cu_{37.6}Al_{8.0}Ag_{8.4}$	2.8×10^{10}	4.8	578	[23]
$Zr_{60.6}Cu_{17.6}Ni_{10.0}Al_{9.8}Fe_{2.0}$	4.9×10^9	14.6	472.8	This work
$Zr_{41.2}Ti_{13.8}Cu_{12.5}Ni_{10}Be_{22.5}$	–	18.5	412.5	[27]
$Zr_{46.75}Ti_{8.25}Cu_{7.5}Ni_{10}Be_{27.5}$	–	26.8	352	[25]

present study are comparable to those determined by viscosity measurements reported in Refs. [25,27]. The discrepancy between the values obtained in the present study and in Ref. [23] is probably due to different definitions of T_g.

The linear thermal expansion coefficients (LTEC) of the as-cast, pre-heated and crystallized $Zr_{45.0}Cu_{39.3}Al_{7.0}Ag_{8.7}$ samples between 325 and 690 K are measured using dilatometry at a heating rate of 0.033 K/s (see Fig. 6). The LTEC of the crystallized sample is found to be 1.18×10^{-5} K^{-1} throughout the investigated temperature range. The LTEC of the as-cast sample within the temperature range from 325 to 425 K 1.30×10^{-5} K^{-1}, which is slightly larger than that of the preheated sample. The LTEC of the as-cast sample decreases in the temperature range from 425 to 650 K because of the structural relaxation, which is due to the annihilation of excess free volume in the sample according to the FVM. The LTEC of the pre-heated sample is measured to be 1.25×10^{-5} K^{-1}, which is almost constant up to 600 K. It can be seen that the LTEC suddenly increases with 0.70×10^{-5} K^{-1} near the glass transition, so the value of the coefficient b is calculated to be 0.107 by substituting the values of D^* and T_0 into Eq. (4).

The results of specific heat capacities (C_p) of the as-cast, pre-heated and crystallized samples measured by DSC are shown in Fig. 7. It can be seen that the C_p of the crystallized sample increases slightly with temperature, whereas the C_p of both the as-cast and pre-heated samples exhibit an abrupt jump near the glass transition. The C_p of the as-cast sample is lower than its crystalline counterpart in the temperature range from 500 to 675 K because of the presence of structural relaxation. It can be determined that the C_p jump near the glass transition is approx 13.5 J/(mol K), corresponding to a β value of 642.1 kJ/mol according to Eq. (5). The physical meaning of β is analogous to the molar formation energy of vacancy in metals, the β value of $Zr_{45.0}Cu_{39.3}Al_{7.0}Ag_{8.7}$ BMG is

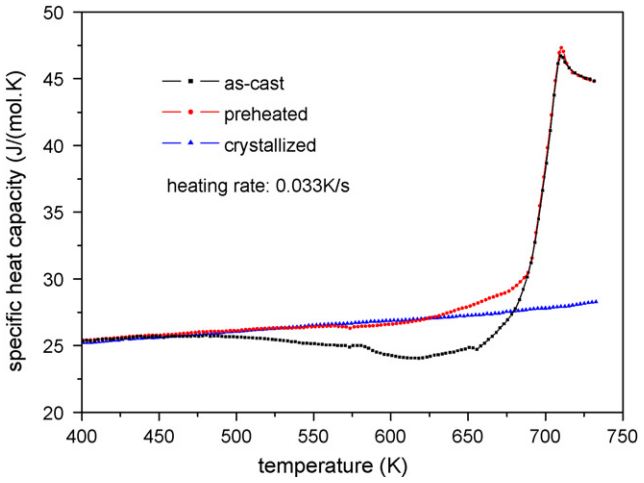

Fig. 7. The specific heat capacities of the as-cast, pre-heated and crystallized $Zr_{45.0}Cu_{39.3}Al_{7.0}Ag_{8.7}$ samples measured by DSC at a heating rate of 0.033 K/s.

Table 3
The values of b, β, D^* and T_0 of $Zr_{45.0}Cu_{39.3}Al_{7.0}Ag_{8.7}$ BMG determined in the present study together with some literature values of different BMGs systems.

BMGs	b	β (kJ/mol)	D^*	T_0 (K)	Reference
$Zr_{45.0}Cu_{39.3}Al_{7.0}Ag_{8.7}$	0.107	642.1	10.3	496.9	This work
$Zr_{41.2}Ti_{13.8}Cu_{12.5}Ni_{10.0}Be_{22.5}$	0.105	–	7.3	672	[27]
$Zr_{46.75}Ti_{8.25}Cu_{7.5}Ni_{10}Be_{27.5}$	–	674.2	26.8	352	[26]
$Zr_{55}Cu_{30}Al_{10}Ni_5$	–	552	–	–	[24]
$Pd_{77.5}Cu_6Si_{16.5}$	0.143	279.7	6.3	505	[6]
$Pd_{40}Cu_{30}Ni_{10}P_{20}$	–	–	20.6	307	[30]
$Pd_{40}Ni_{40}P_{20}$	–	–	18.6	355	[19]
$La_{50}Al_{25}Ni_{25}$	–	386.6	7.1	342	[31]

around 2.8 times larger than the molar formation energy of vacancy in Zr crystals (226 kJ/mol) [29]. However, it is rational since real vacancies in metals usually have half of the atomic volume due to the relaxation of the lattice around the vacancy. In fact, similar ratios have been reported to be 2.5 and 2.1 in the $Zr_{55}Cu_{30}Al_{10}Ni_5$ BMG [27] and $Pd_{77.5}Cu_6Si_{16.5}$ MG [6], respectively. The values of b, β, D^* and T_0 of $Zr_{45.0}Cu_{39.3}Al_{7.0}Ag_{8.7}$ BMG are summarized in Table 3 together with some literature values of different BMG systems.

Fig. 8 shows a representative series of DSC traces of the as-cast and the deformed samples (by cold rolling at a strain rate of 4.6×10^{-3} s^{-1} and by HPT, respectively) measured at 0.33 K/s. It

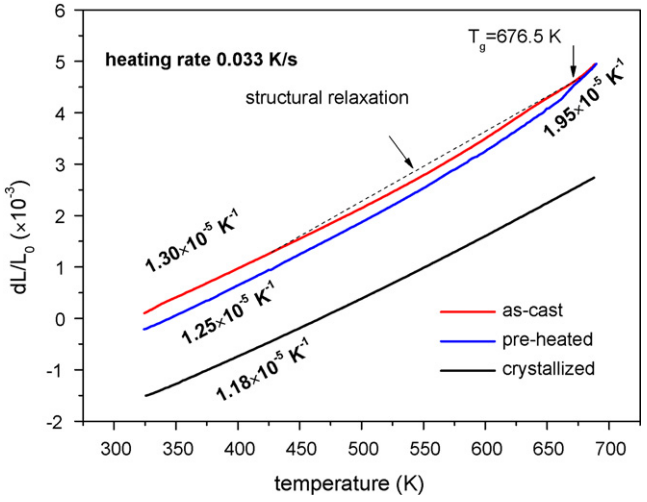

Fig. 6. The linear thermal expansion coefficients of the as-cast, pre-heated and crystallized $Zr_{45.0}Cu_{39.3}Al_{7.0}Ag_{8.7}$ samples determined by dilatometric measurements at a heating rate of 0.033 K/s.

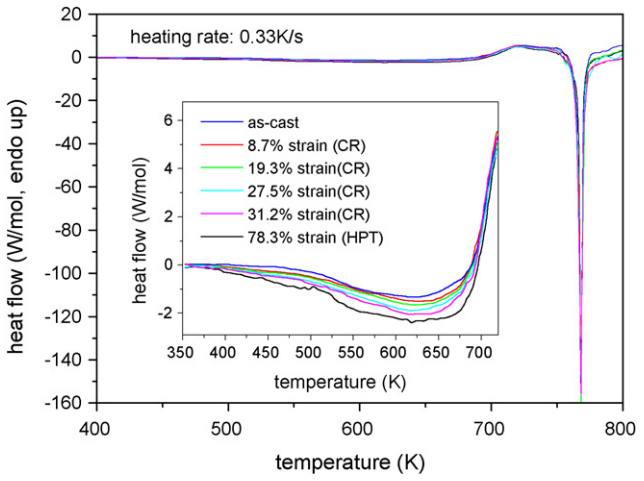

Fig. 8. The DSC traces of the as-cast sample, cold rolled samples at a strain rate of 4.6×10^{-3} s^{-1} and the HPT deformed sample measured at a heating rate of 0.33 K/s, the inset is the enlargement of the structural relaxation range.

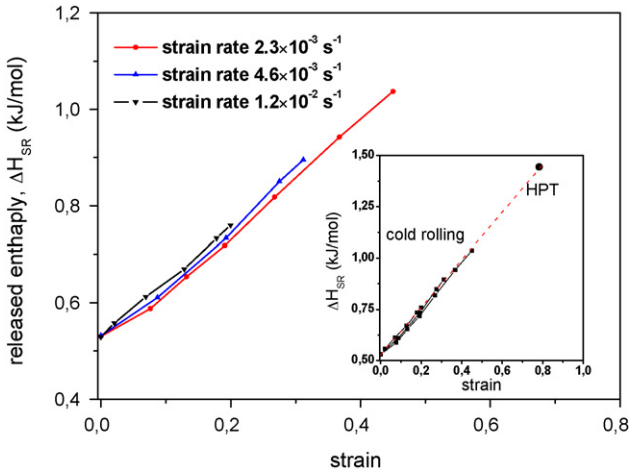

Fig. 9. The released enthalpies ΔH_{SR} during structural relaxation as a function of the deformation strain, the ΔH_{SR} of the sample deformed by HPT falls in the course of the extrapolation of those obtained in the samples deformed by cold rolling (see inset).

can be seen that the amplitudes of the exothermic signals increase with the deformation strains between 350 and 700 K. The released enthalpy ΔH_{SR} is calculated by integrating the area of the exothermic signal (see Fig. 9). It is found that ΔH_{SR} is slightly larger in the samples deformed at higher strain rates than at lower ones by cold rolling. The critical strain ε_c is defined as the maximum strain at which the sample can sustain without fracture during deformation. ε_c is found to be dependent of strain rate in the samples deformed by cold rolling, i.e. ε_c decreases from 0.35 at the strain rate of $2.3 \times 10^{-3}\,s^{-1}$ to 0.20 at the strain rate of $1.2 \times 10^{-2}\,s^{-1}$. The sample deformed by HPT has the largest ΔH_{SR} of 1.44 kJ/mol with $\varepsilon_c = 0.78$ among all the deformed samples. It is also found that the ΔH_{SR} of the sample deformed by HPT falls in the course of the extrapolation of those obtained in the samples deformed by cold rolling.

The absolute contents of free volume are calculated are by the method described Section 2.2 using the equilibrium values of free volume in the temperature range from 740 to 750 K as references. A representative figure of the evolution of free volume in the as-cast and deformed samples with temperature is illustrated in Fig. 10.

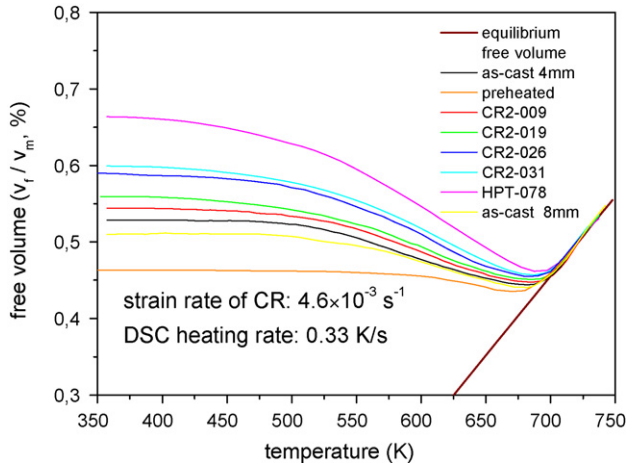

Fig. 10. Evolution of the contents of free volume with temperature in the as-cast and the samples deformed by cold rolling at a strain rate of $4.6 \times 10^{-3}\,s^{-1}$ and by HPT during DSC measurements at 0.33 K/s. ("CR" denotes cold rolling, "CR2-009" denotes the sample deformed by cold rolling with a strain of 9%, the rest may be deduced by analogy.).

Table 4
The absolute contents of free volume (v_f/v_m) of the samples deformed by cold rolling at different strain rates and by HPT.

Deformation method	Strain rate (s^{-1})	Strain	v_f/v_m (%)
Cold rolling	2.3×10^{-3}	0.08	0.543
		0.19	0.561
		0.27	0.594
		0.35	0.609
	4.6×10^{-3}	0.09	0.542
		0.19	0.558
		0.26	0.583
		0.31	0.601
	1.2×10^{-2}	0.06	0.534
		0.13	0.553
		0.18	0.561
		0.20	0.568
HPT	$\sim 1.3 \times 10^{-3}$	0.78	0.672

The absolute content of free volume is given in the form of the ratio of the free volume to the atomic volume of the BMG (v_f/v_m). All the curves shown in Fig. 10 are obtained by averaging three independent measurements, where a scattering of the data within ±0.005% was found. It can be seen that the reduction of free volume starts at approx 500 K in the as-cast sample and shifts to lower temperatures with increasing deformation strain. It can be calculated that v_f/v_m in the as-cast and pre-heated sample under room temperature are 0.533% and 0.476%, respectively. In the deformed samples, v_f/v_m increases monotonously with the deformation strain, the maximum v_f/v_m is found in the samples deformed by HPT to be 0.672%, which is around 1.3 times larger than the v_f/v_m in the as-cast sample. All the v_f/v_m values of the samples deformed by cold rolling at different strain rates are listed in Table 4.

Recently, it was proposed by Gleiter that a new kind of MGs called metallic nanoglasses can be prepared by joining the nanoscaled amorphous particles into bulk glasses [32–34]. The larger amount of excess free volume in nanoglasses compared to conventional MGs can fundamentally change properties of the glass. In the present study, HPT is shown to be able to introduce more excess free volume compared to cold rolling, indicating that HPT may be an alternative approach to produce metallic nanoglasses.

In order to prove the reliability of he values of b, β, D^* and T_0 obtained in the present study, the equilibrium values of free volume between 648 and 684 K were calculated using previous enthalpy

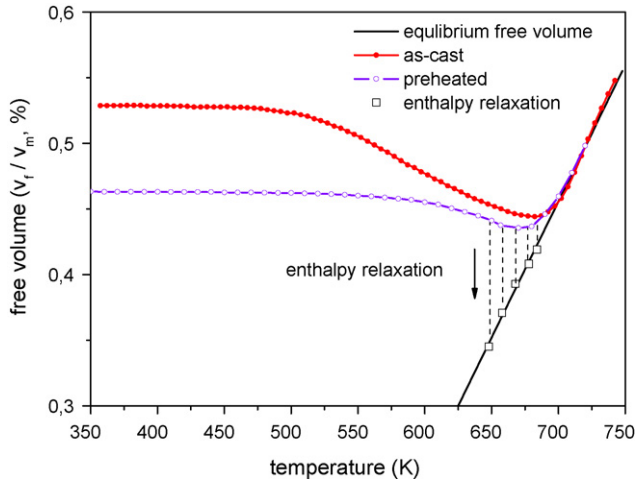

Fig. 11. The equilibrium values of free volume calculated by the parameters (b, β, D^* and T_0) determined in the present study (solid black line) and by the previous enthalpy relaxation measurements (open squares), the good agreement indicates the reliability of the values of these parameters.

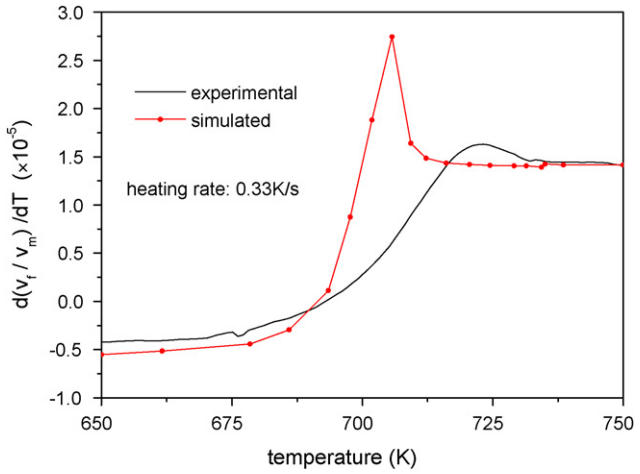

Fig. 12. The experimental (black line) and simulated (red line) DSC curves of the as-cast $Zr_{45.0}Cu_{39.3}Al_{7.0}Ag_{8.7}$ sample at a heating rate of 0.33 K/s (For interpretation of the references to colour in this figure legend, the reader is referred to the web version of the article).

relaxation data [35] and the result is shown in Fig. 11. It can be seen that the calculated equilibrium values of free volume using the relaxed enthalpies and the parameter β are in good agreement with those obtained by Eq. (2) using the values of b, D^* and T_0, indicating that the parameters obtained in the present study are reliable.

It has been previously demonstrated that the DSC traces of some Pd- [6] and Zr-based [36] BMGs upon heating can be simulated using the following flow defect model:

$$\frac{d(v_f/v_m)}{dT} = -\left(\frac{\omega}{\Phi}\right)\cdot\exp\left[\frac{-E}{(RT)}\right]\cdot\left(\frac{vf}{vm}\right)^2 \cdot\left[\exp\left(-\frac{vf}{vm}\right)-\exp\left(-\frac{v_m}{v_{feq}}\right)\right] \quad (7)$$

where ω is a frequency factor, Φ is the heating rate used in DSC, E is an activation energy and v_{feq} is the equilibrium free volume. The best fitting of the experimental DSC data of $Zr_{45.0}Cu_{39.3}Al_{7.0}Ag_{8.7}$ using Eq. (7) yields $E = 180$ kJ/mol and $\omega = 2.6 \times 10^{29}$ s^{-1} (see Fig. 12. However, it can be seen that the fitting quality is far from satisfactory, e.g. the simulated curve shows a steep endothermic peak around glass transition and a large divergence at the end of glass transition. In our opinion, the discrepancy may be resulted from the improperness of the model. In fact, Eq. (7) rises from an assumption that claims the relaxation of flow defects in MGs to be a bimolecular process [37–39]. However, recent enthalpy relaxation experiments on some Pd- and Zr-based BMGs have shown that the isothermal relaxation of BMGs follows the stretched exponential relaxation functions rather than the bimolecular kinetics [28,40].

Finally, it should be mentioned that the free volume quantified in the present study is assumed to be homogenously distributed throughout the investigated samples. Therefore, it is more proper to take the calculated value of free volume as an average. However, real free volume is not homogenously distributed in the samples, especially in the deformed samples, where shear bands are present and the introduced excess free volume is thought to be highly localized in the shear bands. Therefore, the development of new model to describe the structure more realistically is worthy of further investigations.

5. Conclusions

In summary, the absolute contents of free volume in the as-cast, preheated and plastically deformed $Zr_{45.0}Cu_{39.3}Al_{7.0}Ag_{8.7}$ BMG samples were quantified using calorimetric and dilatometric measurements within the framework of the free volume model. The required parameters are experimentally determined to be $b = 0.107$, $\beta = 642.1$ kJ/mol, $D^* = 10.3$ and $T_0 = 496.9$ K, respectively. The good agreement between the equilibrium free volume calculated from previous enthalpy relaxation experiment and this work approved the rationality of the values of these parameters. The content of free volume in the as-cast sample is determined to be 0.533% with respect to the atomic volume of the BMG. Plastic deformations introduce excess free volume in the samples, the introduced excess free volume is found to increase with the deformation strain. The content of free volume in the sample deformed by HPT is quantified to be 0.672%, which is around 1.3 times larger than that of the as-cast sample. The experimental DSC curve is simulated using the flow defect model. Nevertheless, the result indicates that the kinetics of free volume may be more complicated than as described by a bimolecular process.

Acknowledgements

The authors acknowledge the financial support of the Deutsche Forschungsgemeinschaft (DFG) through project Grant No. Al-578-6.

References

[1] D. Turnbull, M.H. Cohen, J. Chem. Phys. 34 (1961) 120–125.
[2] M.H. Cohen, D. Turnbull, J. Chem. Phys. 31 (1959) 1164–1169.
[3] D. Turnbull, M.H. Cohen, J. Chem. Phys. 52 (1970) 3038–3041.
[4] M.H. Cohen, G.S. Grest, Phys. Rev. B 20 (1979) 1077–1098.
[5] F. Faupel, W. Frank, M.P. Macht, H. Mehrer, V. Naundorf, Rev. Mod. Phys. 75 (2003) 237–280.
[6] A. Van den Beukel, J. Siestma, Acta. Metall. Mater. 38 (1990) 383–389.
[7] U. Ramamurty, M.L. Lee, J. Basu, Y. Li, Scr. Mater. 47 (2002) 107–111.
[8] X.J. Liu, G.L. Chen, X. Hui, T. Liu, Z.P. Lu, Appl. Phys. Lett. 93 (2008) 011911.
[9] X.D. Wang, S. Yin, Q.P. Cao, J.Z. Jiang, H. Franz, Z.H. Jin, Appl. Phys. Lett. 92 (2008) 011902.
[10] H.W. Sheng, W.K. Luo, F.M. Alamgir, J.M. Bai, E. Ma, Nature 439 (2006) 419–425.
[11] A.R. Yavari, A.L. Moulec, A. Inoue, N. Nishiyama, N. Lupu, E. Matsubara, Acta Mater. 53 (2005) 1611–1619.
[12] O. Haruyama, Intermetallics 15 (2007) 659–662.
[13] O. Haruyama, A. Inoue, Appl. Phys. Lett. 88 (2006) 131906.
[14] O. Haruyama, H. Sakagami, N. Nishiyama, A. Inoue, Mater. Sci. Eng. A 449–451 (2007) 497–500.
[15] B.P. Kanungo, S.C. Glade, P.A. Kumar, K.M. Flores, Intermetallics 12 (2004) 1073–1080.
[16] K.M. Flores, D. Suh, R.H. Dauskardt, P.A. Kumar, P.A. Sterne, R.H. Howell, J. Mater. Res. 17 (2002) 1153–1161.
[17] K.M. Flores, B.P. Kanungo, S.C. Glade, P.A. Kumar, J. Non-Cryst. Solids 353 (2007) 1201–1207.
[18] M.E. Launey, J.J. Kruzic, C. Li, R. Busch, Appl. Phys. Lett. 91 (2007) 051913.
[19] P. Tuinstra, R.A. Duine, J. Sietsma, A. van den Beukel, Acta. Metall. Mater. 43 (1995) 2815–2823.
[20] D.S. Sung, O.J. Kwon, E. Fleury, K.B. Kim, J.C. Lee, Met. Mater. Int. 10 (2004) 575–579.
[21] Q.K. Jiang, X.P. Nie, Y.G. Li, Y. Jin, Z.Y. Chang, J. Alloys Compd. 443 (2007) 191–194.
[22] G.Q. Zhang, Q.K. Jiang, L.Y. Chen, M. Shao, J.F. Liu, J. Alloys Compd. 424 (2006) 176–178.
[23] Q.K. Jiang, X.D. Wang, X.P. Nie, G.Q. Zhang, H. Ma, H.J. Fecht, Acta Mater. 56 (2008) 1785–1796.
[24] A. Slipenyuk, J. Eckert, Scr. Mater. 50 (2004) 39–44.
[25] A. Masuhr, T.A. Waniuk, R. Busch, W.L. Johnson, Phys. Rev. Lett. 82 (1999) 2290–2293.
[26] E. Bakke, R. Busch, W.L. Johnson, Appl. Phys. Lett. 67 (1995) 3260–3262.
[27] R. Busch, E. Bakke, W.L. Johnson, Acta Mater. 46 (1998) 4725–4732.
[28] I. Gallino, M.B. Shah, R. Busch, Acta. Mater. 55 (2007) 1367–1376.
[29] O.L. Bacq, F. Willaime, A. Pasturel, Phys. Rev. B 59 (1999) 8508–8511.
[30] K. Russew, F. Sommer, J. Non-Cryst. Solids 319 (2003) 289–292.
[31] B.V. Aken, P.D. Hey, J. Sietsma, Mater. Sci. Eng. A 278 (2000) 247–254.
[32] H. Gleiter, Mater. Sci. Forum 584–586 (2008) 41–48.
[33] H. Gleiter, Acta Mater. 56 (2008) 5875–5893.
[34] D. Şopu, K. Albe, Y. Ritter, H. Gleiter, Appl. Phys. Lett. 94 (2009) 191911.

[35] Y. Zhang, H. Hahn, J. Non-Cryst. Solids, Submitted.
[36] P. Wen, M.B. Tang, M.X. Pan, D.Q. Zhao, Z. Zhang, W.H. Wang, Phys. Rev. B 67 (2003) 212201.
[37] S.S. Tsao, F. Spaepen, Acta Metall. 33 (1985) 891–894.
[38] F. Spaepen, Acta Metall. 25 (1977) 407–411.
[39] S.S. Tsao, F. Spaepen, Acta Metall. 33 (1985) 881–884.
[40] T. Zhang, F. Ye, Y.L. Wang, J.P. Lin, Metall. Mater. Trans. A 39 (2008) 1953–1957.